Journal of the European Ceramic Society 22 (2002) 1001–1009

www.elsevier.com/locate/jeurceramsoc

Enhancement of the oxidation resistance of interfacial area in C/C composites. Part I: oxidation resistance of B–C, Si–B–C and Si–C coated carbon fibres

S. Labruquère, H. Blanchard, R. Pailler*, R. Naslain

Laboratoire des Composites Thermostructuraux, UMR 5801 (CNRS-Snecma-UB1), Domaine Universitaire, 3 Allée de La Boétie, 33600 Pessac, France

Received 29 June 2001; accepted 30 July 2001

Abstract

Carbon fibre preforms were coated with B–C, Si–B–C and Si–C deposits obtained by chemical vapour deposition in order to limit their oxidation rate. B–C and B-rich Si–B–C coatings oxidize rapidly and lead to the formation of a glassy film that protect carbon fibres from oxidation. Oxidation occurs by oxygen diffusion through this glassy film. Si–C and Si-rich Si–B–C deposits oxidize slowly and protect efficiently carbon fibre from oxidation. Oxygen accesses to the carbon fibre surface only occurs through cracks of the deposit. Thin deposits (≈30 nm) are less efficient than thicker deposits because the oxygen can progress between SiC crystallites. Deposits thicker than 100 nm efficiently protect carbon fibres from oxidation.

Keywords: Boron-based coatings; C/C composites; Composites; Interfaces; Oxidation protection

1. Introduction

Carbon-based materials exhibit outstanding mechanical properties, particularly at high temperatures. Nevertheless, their prolonged use in oxidising environments is limited to temperatures lower than 500 °C because of gasification of carbon as carbon oxides.[1]

Phosphorus and boron based inhibitors or protective coatings have been proposed to overcome this drawback.[2–5] Boron is known to protect carbonaceous materials by carbon active sites poisoning (for low percentages of boron) or by forming a B_2O_3 film at the surface of the carbonaceous material (for high percentages of boron). The general consensus has been that substitutional boron acts as an inhibitor of carbon oxidation. The following explanations have been proposed:[6] (i) substitutional boron redistributes the π electrons, lowers the Fermi level of graphite and hence presumably inhibits the desorption of CO and CO_2, (ii) substitutional boron enhances the graphitisation of carbon, and (iii) as the carbon is consumed, boron oxide forms on the surface and acts as a diffusional barrier and an active site blocker.

Boron-based CVD coatings have also been proposed to protect carbon materials against oxidation. S. Jacques[7] has shown that the oxidation resistance of C(B) materials obtained by CVD is better than that of pure pyrocarbon. This effect is mainly due to the improvement of the structural organisation of pyrocarbon for the low boron contents and the coating of the whole material with a stable boron oxide for higher boron contents. According to Rodriguez and Baker,[8] such a uniform oxide film is impervious to oxygen attack only below 815 °C, while beyond this temperature boron carbide is formed which acts as an active catalyst of the carbon-oxygen reaction. In the same way, Karra et al.[9] showed that in some cases, boron doping of carbon has a catalytic effect in carbon oxidation, despite the fact that boron lowers the Fermi level and thus presumably decreases the affinity of carbons for oxygen. Further, SiC-B_4C multilayer coatings elaborated by reactive chemical vapour deposition (RCVD) have been reported to increase the oxidation resistance of carbonaceous materials.[10] The use of CVD-coatings such as silicon carbide

* Corresponding author. Tel.: +33-5-56-84-47-18; fax: +33-5-56-84-12-25.

E-mail address: pailler@lcts.u-bordeaux.fr (R. Pailler).

0955-2219/02/$ - see front matter
PII: S0955-2219(01)00410-1

results in the formation of solid silica dioxide between 500 and 1300 °C in the air. This oxidation may generate microcracks through the thin layer, allowing oxygen molecules to diffuse into the carbonaceous substrate.[11,12]

The oxidation resistance can be improved by the use of multiplayer systems that associate pure boron or B_4C or a ternary Si–B–C component with pure SiC. When associated with pure SiC in a sequential manner, the ternary Si–B–C material permit to create a self-protection matrix with improved oxidation resistance when compared to pure SiC, especially under thermo-mechanical stresses.[13,14] The oxidation resistance of such a material is improved in a large range of temperature from 450 to 1500 °C.

The aim of the first part of this work was to study the oxidation resistance of B–C, Si–B–C and Si–C coated carbon fibres and to derive characteristics of the deposit required to protect efficiently carbon fibres from oxidation. The second part is devoted to the study of the oxidation resistance of related C/B–C/C, C/Si–B–C/C and C/SiC/C composites.[15] Finally, in the last part, the mechanical properties of these composites have been assessed before and after oxidation tests.[16]

2. Experimental

2.1. Materials

Experiments were performed on rectangular shape ($0.5\times0.5\times1$ cm^3) N preforms (2D preforms knitted in the third direction) made of PAN fibres (N) from Snecma Moteurs.[1]

The coatings were prepared by Chemical Vapour infiltration (CVI). The experimental apparatus is schematically represented in Fig. 1. The hot-wall reactor is a horizontal silica glass tube (50 mm in inner diameter) heated by a resistive electrical furnace. The total pressure P is maintained in the reactor at a constant value by a vacuum pump through a mechanical regulating system and a pressure gauge. Liquid nitrogen traps permit to condense corrosive by-products. Mass flowmeters are used to control the partial gas flow rates of the precursor components.

H_2 is used as both a carrier gas and a reducing agent. Its flow rate Q (H_2) and the total flow rate of the source gases are fixed for the different experiments. The initial composition is defined by the following ratios:

$$\alpha = 100 \times Q(BCl_3)/(Q(BCl_3) + Q(C_3H_8)) \quad (1)$$

for B–C experiments and

$$\beta = 100 \times Q(BCl_3)/(Q(BCl_3) + Q(MTS)) \quad (2)$$

for Si–B–C experiments, where MTS is the methyltrichlorosilane and $Q\ (i)$ is the gas flow rate of species i. The temperature T is controlled with a Pt/PtRh thermocouple.

Experimental conditions used to produce the deposits are reported in Table 1 and are derived from previous works.[7,17] Deposits I–III referred to B–C deposits (Table 2) and deposits IV–VI referred to Si–B–C deposits. Various initial compositions of the precursor gas mixture were studied. α ratio was chosen within the range 55–85% and β ratio was chosen within the range 33–66% (Table 1).

2.2. Experimental procedures

The deposit thickness, the morphology of the fracture surface and the external surface of the deposits were observed with a high resolution scanning electron microscope (SEM, S4500 from Hitachi).

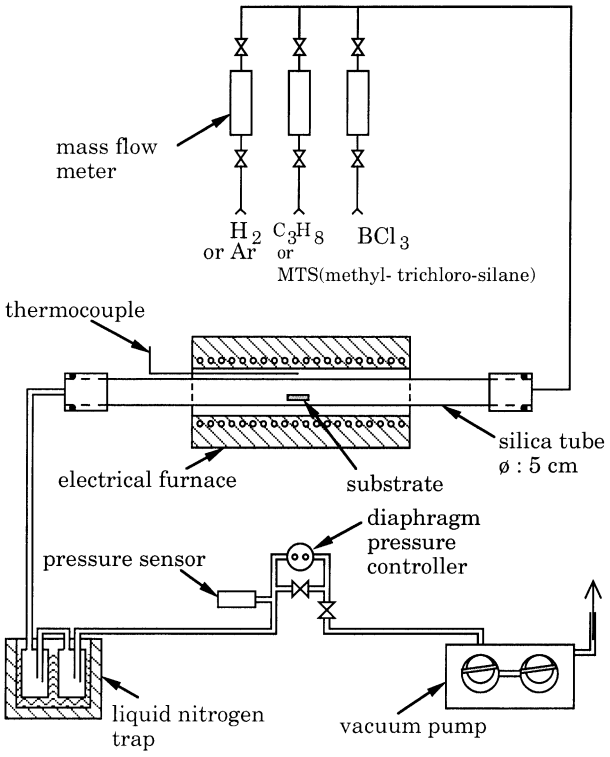

Fig. 1. Apparatus used for the CVI of B–C, Si–B–C and Si–C materials (schematics).

Table 1
Experimental conditions used to produce the deposits

	B–C	Si–B–C	Si–C
H_2 flow rate (cm^3/min)	200	300	40
Total precursor gas flow rate (cm^3/min)	80	60	55
Pressure (kPa)	1	5	3
Nature of gases used	BCl_3–MTS–H_2	BCl_3–C_3H_8–H_2	MTS–H_2

[1] Snecma Moteurs, Le Haillan, France.

The composition of B–C and Si–B–C materials deposited on preforms was determined by Auger electron spectroscopy (AES, VG310F). Conventional elementary trace analyses were carried out on N fibre performs.

Oxidation tests were performed with a Setaram TAG24 thermogravimetric analyser (TGA) under dry air flow (50 ml/min). A 50 °C/min heating rate was used until 650 °C. The temperature was then kept at this value during the oxidation test. The oxidation rate R, is defined as:

$$R = -\frac{1}{m_0}\partial m/\partial t, (\text{expressed in } \% \text{ s}^{-1}) \quad (3)$$

where ∂m is the mass loss observed at time t (when R becomes constant) during a time ∂t for a sample of initial mass m_0.

XRD patterns of finely powdered samples were recorded with a diffractometer (D5000 from Siemens). The average size of the crystallites, L_{111} was calculated from the Scherrer formula:

$$L_{111} = K\lambda/D\cos\theta \quad (4)$$

where K is a constant taken as 0.9, λ the Cu-K_λ wavelength ($\lambda = 0.154$ nm), θ the Bragg angle ($\theta = 017.8°$) and D the width at midheight of the β-SiC (111) peak.

The tensile strength of the monofilaments (coated or not) were tested at room temperature with an apparatus and a procedure which have been described elsewhere.[18] About 20 single fibre specimens were tested at a gauge length $L = 10$ mm. The failure stress was calculated from the load at failure and from the diameter previously measured on each specimen by laser interferometry according to a method described elsewhere. Finally, the Young's modulus of the fibre was calculated from the slope of the stress-strain curve at the origin, taking into account the machine compliance and assuming a linear relationship up to failure.

Table 2
Deposit compositions and experimental conditions used to produce B–C, Si–B–C deposits (boron, carbon and silicon percentages were measured by Auger electron spectroscopy)

Sample	I	II	III	IV	V	VI	Si–C
B (at.%)	18	28	33	50	37	30	0
C (at.%)	82	72	67	41	45	40	55
Si (at.%)				9	18	30	45
α (%)	55	70	85				
β (%)				66	50	33	

Table 3
Atomic concentrations of impurities present in N preforms (as assessed by conventional elementary trace analyses)

Impurities	Ca	Na	Fe	Al	Si	Mg	Cl	Cu	K
At. conc. (ppm)	150	9	10	5.4	5	3.3	40	4.7	2

3. Results

3.1. Chemical analysis

N fibre preforms contain some impurities (Table 3) and principally calcium and sodium which are very active catalytic species.[19]

The boron and silicon contents of the deposits are reported in Table 2. The boron content of C–B materials increases from 18 to 33 at.%.

The boron content of Si–B–C deposits varies from 30 to 50 at.%. Deposits IV and V have a high boron atomic percentage contrary to the deposit VI.

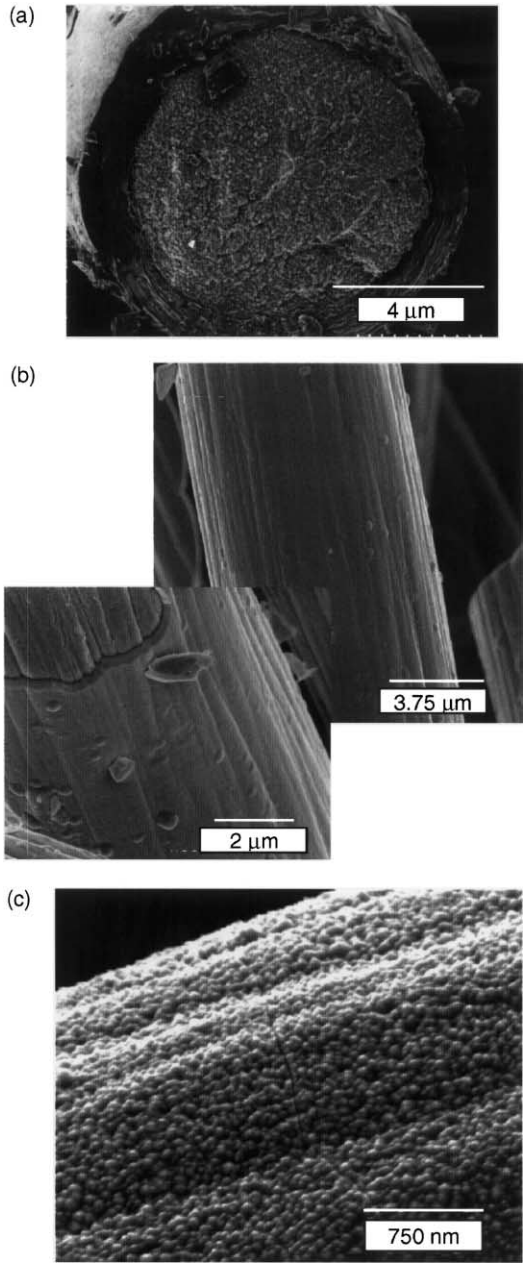

Fig. 2. SEM micrographics showing the external surface of B–C (a), Si–B–C (b) and Si–C (c) coated carbon fibres.

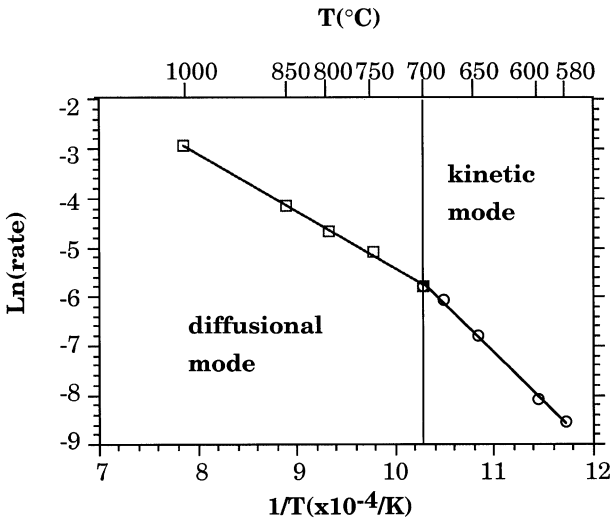

Fig. 3. Arrhenius plot for the oxidation under dry air for N preforms.

The carbon and silicon contents of the Si–C deposit are 55 and 45 at.% respectively. This result is in agreement with that obtained by Yu-Quig et al.[20] in similar CVD conditions.

In the figures, the deposit number is associated with the composition in brackets (Si at.%, B at.%, C at.%)

3.2. Scanning electron microscopy

Morphologies of the various C–B, Si–B–C and Si–C coatings are shown in Fig. 2. The external surface is rather smooth and homogeneous for B–C and Si–B–C deposits though Si–C deposit is rather rough. Moreover cracks of about 30 nm have been observed (Fig. 2c) in the Si–C deposit.

3.3. Structure of coating

For Si–C coatings, the XRD pattern only shows peaks of α-SiC and β-SiC. The calculated average size of the crystallites is about 39 nm for a deposit of 250 and 10 nm for a deposit of 30 nm. All the other coatings (B–C and Si–B–C) are amorphous.

3.4. Thermogravimetric experiments

In order to choose an oxidation temperature, the thermal variations of the oxidation rate, R for the N fibre performs are shown, as an Arrhenius plot, in Fig. 3 (R being constant). From the values of the related apparent activation energies, it is assumed that oxidation is controlled by reaction kinetics for $T<700$ °C. Two oxidation temperatures were chosen: 650 and 1000 °C in order to study kinetic and diffusional rate-controlled phenomena, respectively.

3.4.1. Kinetic phenomena

The mass variations $\Delta m/m_0$ of B–C coated fibre performs are shown in Fig. 4 as a function of the oxidation time, t. A rapid mass loss is observed at the beginning of the oxidation test. As expected, the mass loss decreases,

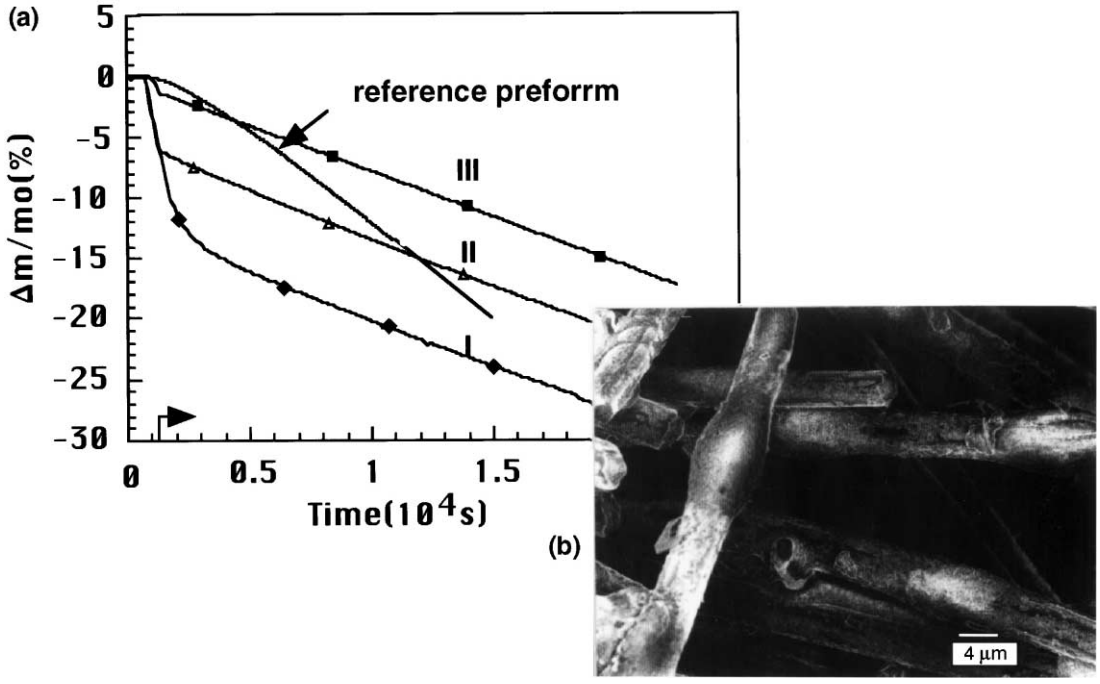

Fig. 4. (a) Thermogravimetric analysis conducted at 650 °C under dry air flow for N preforms coated with B–C deposits [deposit numbers are indicated on the curves with respective Si/B/C content in at.%—I: (0/33/67); II: (0/28/72); III: (0/18/82)] and (b) aspect of coated fibres after oxidation (2×10^4 s). (► A temperature of 650 °C is first obtained and the temperature is then maintained at this value.)

for a given oxidation time, when the boron content of the B–C deposit increases. Further, a SEM micrograph of an oxidized coated B–C fibre shows a glassy film of B_2O_3 at the surface of carbon fibres (Fig. 4b).

The variations of the oxidation rates of carbon fibres coated with B–C deposits of different thickness are reported in Fig. 5 as a function of the oxidation time: the thicker the B–C deposit, the better the oxidation resistance of the coated preform.

The TGA curves for Si–B–C and Si–C coated (250 nm) fibres are shown in Fig. 6. A large mass gain is observed at the beginning of the oxidation test essentially for B-rich Si–B–C coated carbon fibres. For sample VI which is very rich in silicon, a slight mass gain is observed during the entire oxidation test. For boron-rich Si–B–C deposits, the stabilized oxidation rate of coated preforms is 6 times lower than the oxidation rate of uncoated one. A SEM micrographs of Si–B–C coated fibres after the oxidation test is shown in Fig. 7. Two kinds of phases are present at the fibre surface: a glassy phase that tends to cover the carbon fibre and crystalline species. TGA tests carried out on Si–C coated (250 nm) carbon fibres (Fig. 6) show an important improvement of the oxidation resistance (the oxidation rate of Si–C coated carbon preforms is reduced by a factor of ≈60). AES data show that a very thin layer of SiO_2 (3 nm) was formed at the surface of the coating.

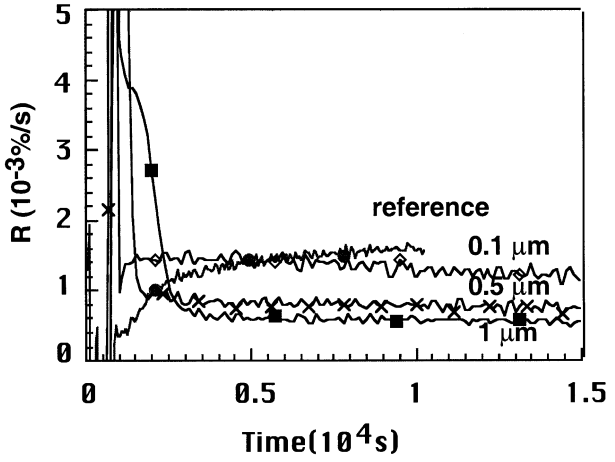

Fig. 5. Oxidation rates of B–C coated fibres (III) (0/33/67), with coatings of different thicknesses.

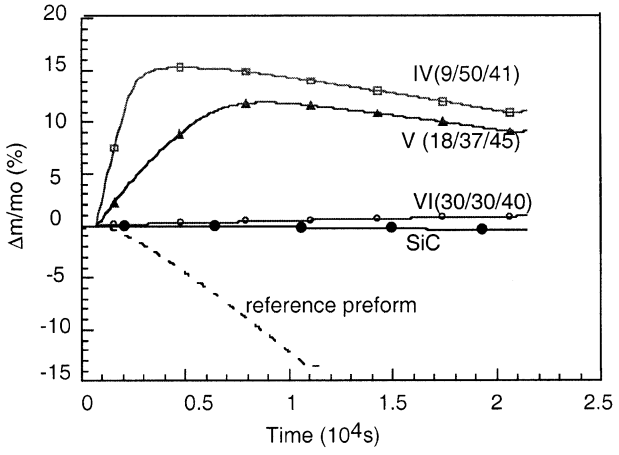

Fig. 6. Thermogravimetric analyses conducted at 650 °C under dry air flow for N preforms coated with Si–B–C deposits (deposit numbers and composition are indicated on the curves).

3.4.1.1. Influence of the Si–B–C deposit thickness on the oxidation resistance. The mass variations of coated Si–B–C carbon fibres versus time for three coating thicknesses i.e. 30, 100 and 250 nm, are shown in Fig. 8.

It clearly appears that for boron-rich Si–B–C coated carbon fibres, the thicker the deposit, the greater the mass increase observed at the beginning of the oxidation test. Oxidation rate of coated preforms slightly decreases when Si–B–C deposit thickness increases. The oxidation rates of silicon-rich Si–B–C coated fibres are very low for deposits thicker than 100 nm. For thinner deposits (30 nm) oxidation protection is not so efficient.

3.4.2. Diffusional phenomena (T = 1000 °C)

Thermogravimetric tests were carried out at 1000 °C for different coated carbon fibres (Fig. 9). A mass gain is observed at the beginning of the boron-rich Si–B–C coated fibre oxidation test. Then, the oxidation rate of the coated perform is divided by 2 compared to the untreated perform.

Silicon-rich and Si–C coatings protect efficiently carbon fibres from oxidation. The time necessary to oxidize a Si–C coated carbon fibre (at 50 mass % loss), is 50 times longer than that required to oxidize an uncoated carbon fibre.

Oxidation rates of carbon fibres coated with silicon-rich Si–B–C and Si–C deposits are reported in Fig. 10.

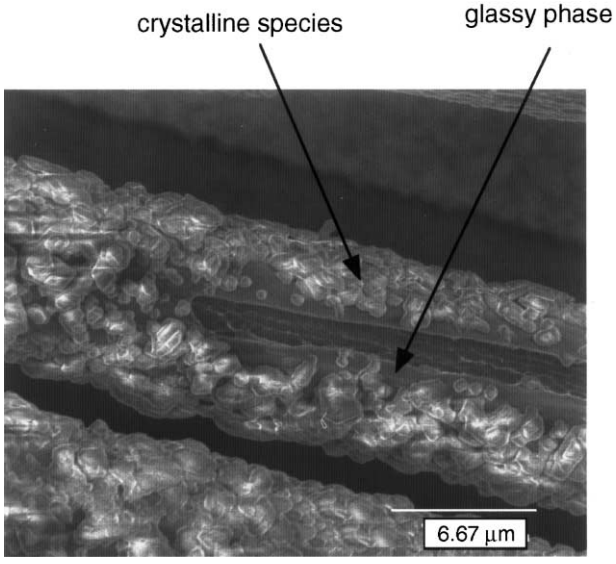

Fig. 7. Scanning electron micrograph of a silicon-rich Si–B–C (IV:50/41/9) coated fibre after an oxidation test at 650 °C (2×10^4/s).

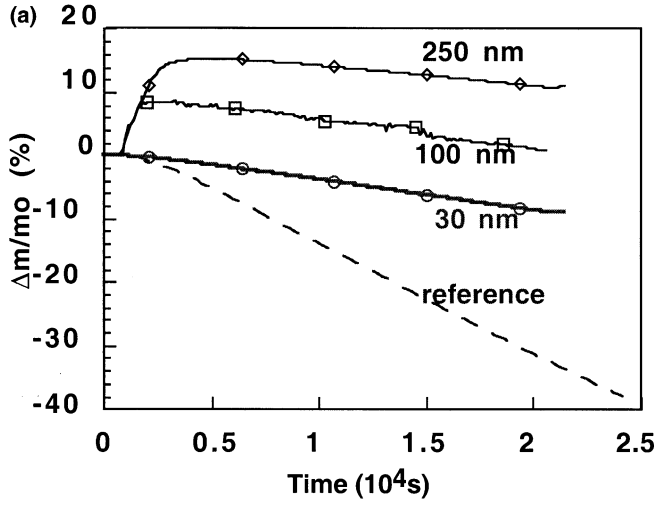

	R (10^{-4}%/s)
250 nm	3.5
100 nm	4.2
30 nm	4.8
reference	17.5
10^4s<t<2x10^4s	

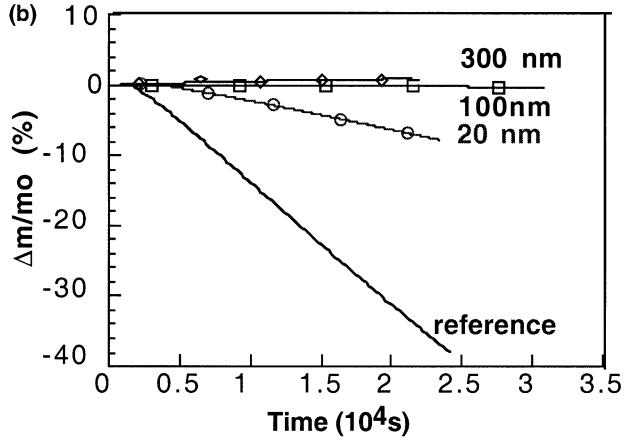

	R (10^{-4}%/s)
250 nm	0
100 nm	0
30 nm	4.2
reference	17.5
10^4s<t<2x10^4s	

Fig. 8. Thermogravimetric analyses conducted at 650 °C under dry air flow for N preforms coated with boron-rich Si–B–C deposits (IV:50/41/9) (a), silicon-rich Si–B–C deposits (VI:30/30/40) (b).

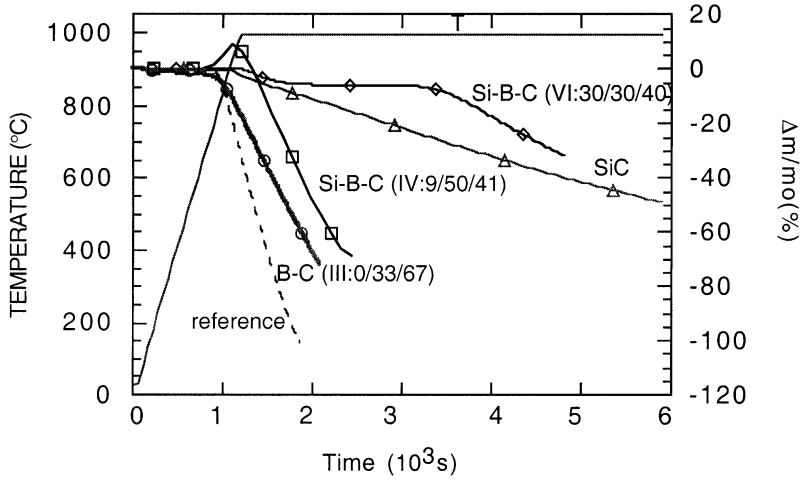

Fig. 9. Thermogravimetric analyses conducted at 1000 °C under dry air flow for N preforms coated with B–C, Si–B–C and Si–C deposits (deposit numbers and compostition are indicated on the curves).

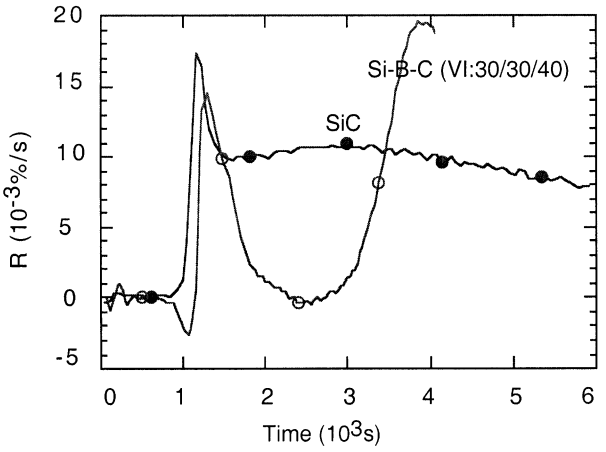

Fig. 10. Oxidation rate of silicon-rich Si–B–C (VI:30/30/40) and Si–C coated carbon fibres. Thermogravimetric tests were carried out at 1000 °C under dry air flow.

As the temperature increases, oxidation rates of Si–C and silicon-rich Si–B–C coated carbon fibres increase rapidly up to 0.018%/s. At about 1500 s from the beginning of the oxidation test, oxidation rates of coated carbon fibre decrease. For the Si–C-coated fibres a 0.01%/s oxidation rate is observed and the oxidation rate remains stable at about this value during the oxidation test. For the silicon-rich Si–B–C coated carbon fibres, oxidation rate decreases rapidly beyond about 2000 s from the beginning of the oxidation test. Oxidation rate stays stable during about 1000 s at about 0%/s and then increases rapidly up to 0.02%/s.

SEM observation carried out at the end of the oxidation test on the Si–C oxidized coated carbon fibres shows the formation of hollow tubes (Fig. 11). The Si–C hollow tubes are coated with a smooth and continuous oxide scale whose thickness is constant along their whole cross-section.

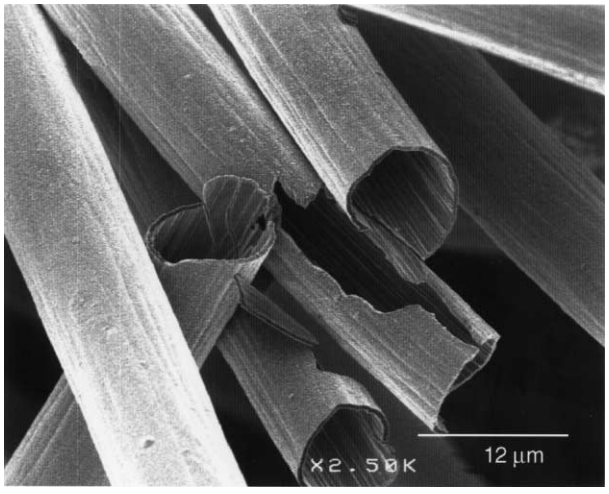

Fig. 11. Surface of Si–C coated carbon fibres after an oxidation test at 1000 °C during 3 h.

For Si–C deposits, the silica thickness growth obeys a parabolic law at 1000 °C, which can be written as:

$$e^2(t) - e_o^2 = K_T.t \quad (5)$$

where K_T is the kinetic constant and e_o is the silica layer for $t=0$.

The silica thicknesses were directly measured by SEM after the total oxidation of carbon fibres. K_T and e_o were derived from these data ($e_o=0$ nm, $K_T=0.098$ nm^2/s). After 1500 s of oxidation a ≈39 nm SiO_2 film is formed on the Si–C coating.

3.5. Mechanical behaviour of coated carbon fibres

It is well known that the ultimate tensile strength, σ^r, of carbon fibres decreases when they are coated with a brittle material of a lower tensile failure strain: the thicker the deposit the lower the mechanical properties of carbon fibres.[21] The aim of this paragraph is to determine if in our case the mechanical properties decrease is due to a chemical degradation of the fibre during the deposit or to a fragile failure of the deposit.

Assuming that a crack equivalent to the deposit thickness c occurs along the direction normal to the loading one, the infinitely-remote tensile stress ${}^r\sigma^r$ acting on the fibre is given by:[22,23]

$$\sigma = YKK_I/\sqrt{\pi c} \quad (6)$$

where Y and K are constants and K_I is the mode I stress intensity factor. The variations of σ^r versus the square root of the inverse of deposit thickness ($1/\sqrt{c}$) are shown in Fig. 12. σ^r is indeed proportional to $1/\sqrt{c}$ and then the coating thickness seems to be the major parameter

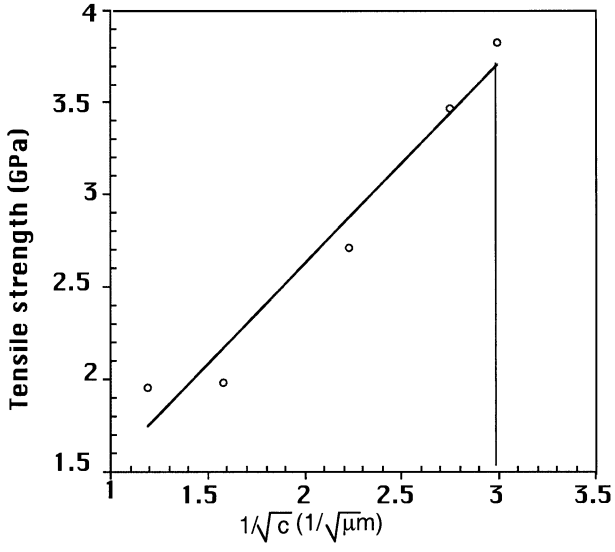

Fig. 12. Tensile strength versus the inverse of the square root of the deposit thickness.

controlling the ultimate tensile stress of the coated fibre. The last point shown on the graph corresponds to the tensile strength of the fibre without coating and it fits with the other points. An average value of the intrinsic defect size of the carbon fibre has been derived from these data. It is of the order of 11 nm.

4. Discussion

4.1. Kinetic mode of oxidation (T = 650 °C)

4.1.1. B–C coated preforms

A rapid mass loss is observed at the beginning of oxidation tests of B–C coated carbon fibres which can be assigned to a rapid oxidation of the B–C coating. The B–C coating oxidation leads to the formation of liquid boron oxide with and evolution of CO_2. Mass gain due to B_2O_3 formation is lower than mass loss due to CO_2 evolution for deposits I and II. Moreover, the total mass loss that would be observed at the end of the deposit oxidation was calculated taking into account the deposit mass and its atomic composition (Table 4). It appears that the calculated mass loss corresponds to the mass loss observed at the beginning of the oxidation test. The B–C deposit is totally oxidised at the beginning of the oxidation test.

The oxidation rate of the B–C deposit is very high compared to the carbon fibre oxidation rate. The boron present in the deposit seems to accelerate carbonaceous material oxidation. Karra et al.[9] showed that in some cases, boron doping of carbons was found to have a catalytic effect in carbon oxidation.

The rapid oxidation rate of the deposit leaves a B_2O_3 film at the surface of fibres that limits carbon fibre oxidation rate. Hence, the oxidation resistance of B–C coated carbon fibres is dependent on B_2O_3 film thickness that is to say on boron content and thickness of the deposit. The oxidation rate of carbon fibre preforms containing 18 or 28 wt.% of boron is higher than the oxidation rate of preforms containing 33 wt.% of boron (Fig. 4) and the thicker the deposit, the lower the oxidation rate (Fig. 5).

Only deposits with very high boron concentration will be interesting to protect efficiently carbon fibres from oxidation.

4.1.2. Si–B–C and Si–C coated carbon preforms

Si–B–C and Si–C deposit oxidation results in a mass increase. But the oxidation rates of the different deposits are very different and increase with the boron content of the deposit.

Boron-rich Si–B–C deposit oxidation occurs at the beginning of the oxidation test and leads to the formation of a glassy film. Oxidation of carbon fibres occurs by oxygen diffusion through this glassy film.

For silicon-rich Si–B–C and Si–C deposits oxidation is slow. Deposits block the access of oxygen to the carbon fibres surface. For the Si-rich Si–B–C coated preform, a slight mass increase is observed during the oxidation test. It corresponds to the slow oxidation of the Si–B–C deposit. On the contrary, a slight mass loss is observed during the Si–C-coated fibres oxidation. The mass increase due to Si–C deposit oxidation is lower than the mass decrease due to carbon oxidation occurring at microcracked zones. Indeed, cracks of about 30 nm (Fig. 2) have been observed at the Si–C deposit surface.

Thin deposits of Si–C or Si-rich Si–B–C are less efficient than larger deposits because oxygen can progress between Si–C crystallites. 30 nm-Si–C coatings are constituted of 10 nm Si–C crystallites (as established by X-ray diffraction). On the contrary, for thicker deposits (a 250 nm deposit is constituted of 39 nm Si–C crystallites) oxygen progression is stopped before the surface of carbon fibres.

4.2. Diffusional phenomena (T = 1000 °C)

For B-rich Si–B–C and B–C deposits, oxygen diffusion rate through the glassy deposit increases rapidly with the temperature and is very important at 1000 °C. Moreover beyond 1000 °C the vapour pressure of B_2O_3 becomes important[24] and B_2O_3 could react with carbon fibres. B–C and boron-rich Si–B–C deposits result in a decrease of the oxidation rate by a factor of 2 but no longer protect efficiently carbon fibres at 1000 °C.

Table 4
Mass variations calculated or observed after the total oxidation of the B–C deposit

Deposit number	I	II	III
Carbon preform mass (mg)	216.2	170	99
B–C deposit mass (mg)	69.2	51	28.7
B wt.% in the deposit	16.5	25.9	32.6
B_2O_3 film mass (mg)[a]	36.8 (17%)	42.6 (24%)	30.2 (30%)
Mass gain after the total oxidation of the deposit	−11.4	−4	+1.13
Mass gain observed[b]	−14	−7	−1

[a] It corresponds to the mass of the B_2O_3 film formed if the B–C deposit is totally oxidized. The brackets indicate the percentage of the B_2O_3 film mass compared to the preform mass.

[b] Mass gain observed after the rapid oxidation observed at the beginning of the oxidation test.

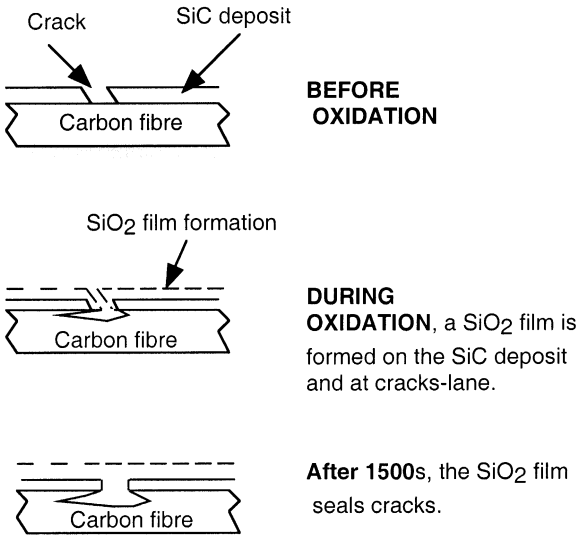

Fig. 13. Scheme showing the evolution of Si–C coated carbon fibres during an oxidation test.

Silicon-rich Si–B–C and Si–C deposits are more efficient. Deposit oxidation rate is slow and oxygen access to the carbon fibre is delayed (Fig. 13). At the beginning of the oxidation of Si-rich Si–B–C coated perform, a mass increase is observed (Fig. 10). It corresponds to a rapid oxidation of the surface of the deposit. Mass gain due to the deposit oxidation is higher than mass loss due to carbon fibre oxidation through cracks of the deposit. Then, oxidation rates of Si–B–C and Si–C coated preforms increase rapidly. Oxidation occurs at deposit cracks level: the longer the oxidation time, the higher the oxidation rate of carbon fibres trough the cracks of the deposit and the thicker the SiO_2 film formed.

After 1500 s of oxidation at 1000 °C, for Si–C coated preforms, a 40 nm SiO_2 film is formed at the surface of the Si–C deposit. Cracks are sealed and oxidation rate of the coated preform decreases. Then, the oxidation rate decreases slightly due to an increase of the SiO_2 film, and so a decrease of the oxygen diffusion rate at sealed cracks zones.

For Si–B–C coated preforms, after 1500 s of oxidation, deposit cracks are sealed. The oxidation rate is about 0%/s meaning that mass gain due to the deposit oxidation is equal to the mass loss due to carbon fibres oxidation. After 3000 s, the Si–B–C deposit is totally oxidized and oxidation occurs through the glassy film formed by oxidation of the deposit.

5. Conclusion

B–C and boron-rich Si–B–C deposits oxidize rapidly and lead to the formation of a glassy film. Oxidation occurs by oxygen diffusion through this glassy film: the higher the oxidation temperature, the more rapid the oxygen diffusion through the glassy film, and the worse the protection of the deposit. Moreover, it was observed that the thicker the deposit, the slower oxygen diffusion rates through the deposit and the better deposit protection. In all cases, this kind of deposit does not protect efficiently carbon fibres from oxidation.

Si–C and silicon-rich Si–B–C deposits (100 nm) oxidize slowly and protect efficiently carbon fibres from oxidation: the higher the silicon content on the deposit, the slower the deposit oxidation and the better the oxidation resistance.

In order to protect efficiently carbon fibres from oxidation, deposits have to: (i) oxidize very slowly, (ii) undergo no chemical reaction with carbon fibres, and (iii) be not too thick in order to keep good mechanical properties and not too thin to protect efficiently carbon fibres from oxidation.

Acknowledgements

This work has been supported by CNRS and Snecma through a grant to S.L. The authors are indebted to J.M. Jouin and J. Thébault from Snecma Moteurs for assistance and valuable discussion.

References

1. Sheehan, J. E., Oxidation protection for carbon fiber composites. *Carbon*, 1989, **27**(5), 709–715.
2. Magne, P., Amariglio, H. and Duval, H., Etude cinétique de l'oxydation du graphite inhibée par les phosphates. *Bull. Soc. Chim. France*, 1971, **6**, 2005–2010.
3. McKee, D. W., Borate treatment of carbon fibers and carbon–carbon composites for improved oxidation resistance. *Carbon*, 1986, **24**(6), 737–741.
4. McKee, D. W., Spiro, C. L. and Lamby, E. J., The effects of boron additives on the oxidation behavior of carbons. *Carbon*, 1984, **24**(6), 507–511.
5. Erburger, P., Baranne, P. and Lahaye, J., Inhibition of the oxidation of carbon-carbon composite by boron oxide. *Carbon*, 1986, **24**(4), 495–499.
6. Jones, L. E. and Thrower, P. A., *Carbon*, 1991, **29**(2), 251.
7. Jacques, S., Guette, A., Langlais, F. and Naslain, R., *Mater. J. Sci.*, 1997, **32**, 983–988.
8. Rodriguez, N. M. and Baker, R. T. K., Fundamental studies of the influence of boron on the graphite-oxygen reaction using in situ electron microscopy techniques. *Mater. J. Res.*, 1993, **8**(8), 1886–1894.
9. Karra, M., Zaldivar, R.J., Rellick, G.S., Thrower P.A. and Radovic, L.R., Substitutional boron in carbon oxidation: inhibitor or catalyst?
10. McKee, D. W., *Carbon*, 1987, **25**, 551.
11. Gray, P. E., US Patent 4 894 286, 1990.